Electronic Supplementary Information (ESI) for:

Regulating charge distribution of Cu_3PdN nanocrystals for nitrate electroreduction to ammonia†

Kai Yao,[a] Zhaobin Fang,[a] Jieyue Wang,[a] Wenhai Wang,[a] Mingyue Wang,[a] Weijie Yan,[a] Mingfu Ye,[a] Binbin Jiang,*[c] Konglin Wu,*[a,b,d] and Xianwen Wei*[a]

[a] *Engineering Research Center of Biofilm Water Purification and Utilization Technology of Ministry of Education, Anhui University of Technology, Maanshan 243032, China.*

[b] *Anhui Laboratory of Molecule-Based Materials, College of Chemistry and Materials Science, Anhui Normal University, Wuhu 241002, China.*

[c] *School of Chemistry and Chemical Engineering, Anqing Normal University, Anqing 246001, China.*

[d] *Institute of Clean Energy and Advanced Nanocatalysis (iClean), Anhui International Joint Research Center for Green Manufacturing and Biotechnology of Energy Materials, School of Chemistry and Chemical Engineering, Anhui University of Technology, Maanshan 243032, China.*

Corresponding authors:

E-mails: klwuchem@ahut.edu.cn or konglin@mail.ahnu.edu.cn (K. Wu);

xwwei@ahut.edu.cn (X. Wei);

bbjiang0726@126.com (B. Jiang).

1. Experimental section

1.1 Chemicals and materials

Copper(II) nitrate trihydrate ($Cu(NO_3)_2 \cdot 3H_2O$), oleylamine, and 1-octadecene were purchased from Sigma-Aldrich. Palladium(II) acetylacetonate ($Pd(acac)_2$) was purchased from Alfa Aesar. Oleylamine and octadecene were degassed prior to used, and all other chemicals were used as received without further purification. All syntheses were carried out under Ar using standard Schlenk techniques, and the workup procedures were performed in air.

1.2 Synthesis of Cu_3PdN and Cu_3N

$Cu(NO_3)_2 \cdot 3H_2O$ (60 mg) and $Pd(acac)_2$ (25.2 mg) were dissolved in 7.5 mL of 1-octadecene and 2.5 mL of oleylamine. The solution was then transferred to a 100 mL three-necked round-bottom flask fitted with a condenser, thermometer adapter, thermometer, and rubber septum and was degassed under vacuum at 120 °C for 10 min. The flask was then filled with argon, heated to 240 °C, and kept at this temperature for 15 min. The flask was then removed from the heating mantle and allowed to cool to room temperature.[1] A solid was precipitated by adding 25 mL of ethanol and then centrifuging at 10000 rpm for 5 min. The product was washed three times by using a 1:1 toluene/ethanol mixture. By the same method, the Cu_3N nanoparticles were obtained without $Pd(acac)_2$.

1.3 Synthesis of Cu_3PdN-300/AC and Cu_3N-300/AC

The achieved Cu_3PdN (or Cu_3N) was dispersed in cyclohexane by ultrasonication to form a homogeneous solution. The obtained above dispersion was added in 50 mL carbon black (2 $mg \cdot mL^{-1}$) dropwise with continuous ultrasonication and following stirring for 24 h. Subsequently, the achieved powder was washed with cyclohexane and ethanol, respectively. Then, the achieved power was dried in a vacuum drying oven at 30 °C. The lastly, the achieved power was annealed at 300 °C for 3 h at Ar atmosphere and named as Cu_3PdN-300/AC. By the same process, the Cu_3N-300/AC was obtained. In addition, other Cu_3PdN-200/AC, Cu_3PdN-400/AC and Cu_3PdN-500/AC samples at different annealing temperatures (such as 200 °C, 400 °C and 500 °C, respectively) were prepared by using the same method described above.

1.4 Characterization

The structure and morphology were characterized by X-ray powder diffraction (XRD, Rigaku Ultima IV), Transmission electron microscopy (TEM, Hitachi H-7700), high resolution TEM (HRTEM), high angle annular dark field scanning transmission electron microscopy (HAADF-STEM) and elemental mapping by energy-dispersive X-ray spectrometry (EDS, JEOL JEM-2100F), X-ray photoelectron spectroscopy (XPS, Thermo Fisher Scientific ESCALAB 250Xi). The metal contents in achieved product were detected by ICP-OES (Agilent 720). The products were determined by Nuclear magnetic resonance hydrogen spectrum (^{1}H NMR, AVANCE 400).

2 Electrochemical measurements

2.1 Preparation of Cu_3PdN-300/AC (or Cu_3N-300/AC) electrode

Typically, 2 mg of Cu_3PdN-300/AC (or Cu_3N-300/AC) and 10 μL of Nafion (5wt%) were scattered in a mixture of 200 μL water and 100 μL anhydrous alcohol by ultrasonic treatment for 30 mins to form a homogeneous liquid. Then, 30 μL of suspension was added on carbon cloth (0.5×0.5 cm^2) and dried at natural atmosphere, and the Cu_3PdN-300/AC (Cu_3N-300/AC) electrode. The preparation of the Cu_3PdN-300/CP (Cu_3N-300/AC/CP) electrode is the same as that of Cu_3PdN-300/AC electrode.

2.2 Electrochemical nitrate reduction experiment

Electrochemical measurements were tested by a CHI 660E electrochemical workstation. A typical H-type electrolytic cell separated by a membrane was employed. The catalyst located on carbon paper, saturated Ag/AgCl electrode and platinum wire respectively as the working electrode, reference electrode and counter electrode. The surface area of the working electrode was controlled with 0.25 cm^2. 1.0 $g \cdot L^{-1}$ Na_2SO_4 solution (30 mL) was distributed to the cathode and anode compartment. $NaNO_3$ was added into the cathode compartment for NO_3^- reduction (containing 50 ppm nitrate-N). All potentials were recorded against the reversible hydrogen electrode (RHE). All the polarization curves were the steady lines after continuous cycles, and the current density was normalized to the geometric. The liner sweep voltammetry was performed at a rate of 10 $mV \cdot s^{-1}$, and the potentiostatic test

was conducted at the different potential for 3 h at a stirring rate of ~300 rpm. For the stability test, the same piece of catalysts undergoes the above process eight times. The double-layer capacitance was evaluated at overpotential from -0.25 V to -0.35 V vs. RHE at different scan rate in 1.0 $g \cdot L^{-1}$ Na_2SO_4 solution.

3 Determination of ion concentration

The ultraviolet-visible (UV-Vis) spectrophotometer was used to detect the ion concentration of pre- and post-test electrolytes after diluting to appropriate concentration to match the range of calibration curves. The specific detection methods are as follow:

3.1 Determination of nitrate-N

Firstly, 1.0 ml electrolyte was taken out from the electrolytic cell and diluted to 5 ml to the detection range. Then, 0.1 mL 1 M HCl and 0.01 ml 0.8 wt% sulfamic acid solution were added into the aforementioned solution. The absorption spectrum was measured using an ultraviolet-visible spectrophotometer and the absorption intensities at a wavelength of 220 nm and 275 nm were recorded. The final absorption value was calculated by this equation: $A = A_{220nm} - 2A_{275nm}$. The concentration-absorbance curve was calibrated using a series of standard potassium nitrate solutions and the potassium nitrate crystal was dried at 105 ~ 110 °C for 2h in advance.

3.2 Determination of nitrite-N

The color developer was configured as follows: *p*-aminobenzenesulfonamide (20 g) was added to a mixed solution of 250 mL of ultrapure water and 50 mL of phosphoric acid (ρ=1.70 $g \cdot mL^{-1}$), and then N-(1-Naphthyl)ethylenediamine dihydrochloride (1.0 g) was dissolved in the above solution. Finally, the above solution was transferred to a 500 mL volumetric flask and diluted to the mark. 1.0 mL electrolyte was taken out from the electrolytic cell and diluted to 5 mL to detection range. Next, 0.1 mL color reagent was added into the aforementioned 5 mL solution. After shanking and standing for 20 minutes, the absorbance was tested by UV-Vis spectrophotometry at a wavelength of 540 nm. The concentration-absorbance curve was calibrated using a series of standard sodium nitrite solutions.

3.3 Determination of ammonia-N

The produced ammonia was spectrophotometrically determined by the indophenol blue method. Typically, 1.0 mL electrolyte was taken out from the electrolytic cell and diluted to 5 mL to the detection range. Afterwards, 2 mL of 1.0 M NaOH solution containing 5 wt% salicylic acid and 5 wt% sodium citrate was added, followed by 1 ml NaClO solution (0.05 M) and 0.2 mL of an aqueous solution of sodium nitroferricyanide (1 wt%) were added. After standing at room temperature for 2h, the UV-Vis absorption spectrum was collected at a wave-length of 655 nm. The concentration-absorbance curve was calibrated by using standard NH_4Cl solution for a series of concentrations. The concentration-absorbance curve was calibrated can be obtained through different concentrations of NH_4Cl solutions and the NH_4Cl chloride crystal was dried at 105 °C for 2 h in advance.

3.4 Calculation of the yield, selectivity, and Faradaic efficiency

The potential (versus saturated Ag/AgCl) was converted to RHE using the following equations:

$$E_{RHE} = E_{Ag/AgCl} + 0.0592\ pH + E^0_{Ag/AgCl}$$

The conversion of NO_3^- was calculated using the equations:

$$C_{NO_3^-} = \Delta C_{NO_3^-} / C_0 \times 100\%$$

The selectivity of the product calculated using the equations:

$$S_{NO_2^-} = C_{NO_2^-} / \Delta C_{NO_3^-} \times 100\%$$

$$S_{NH_3} = C_{NH_3} / \Delta C_{NO_3^-} \times 100\%$$

The yield rate of NH_3 was calculated using the equations:

$$Y_{NH_3} = (C_{NH_3} \times V) / (t \times m_{cat})$$

The Faradaic efficiency was calculated using the equations:

$$FE_i = (n_i \times z_i \times F) / Q \times 100\%$$

Where $E^0_{Ag/AgCl}$ = 0.197 V, C_0 is the initial concentration of NO_3^-, C_{NH_3} is the measured NH_3 concentration ($mol \cdot L^{-1}$), V is the electrolyte volume of cathode cell, t is the electrolysis time, m_{cat} is the mass of catalyst, n_i is the amount of product i (mol), z_i is the number of electrons transferred to product i, F is the Faradaic

constant (96,485 C mol^{-1}), Q is the total charge (C) passing the electrolytic cell.

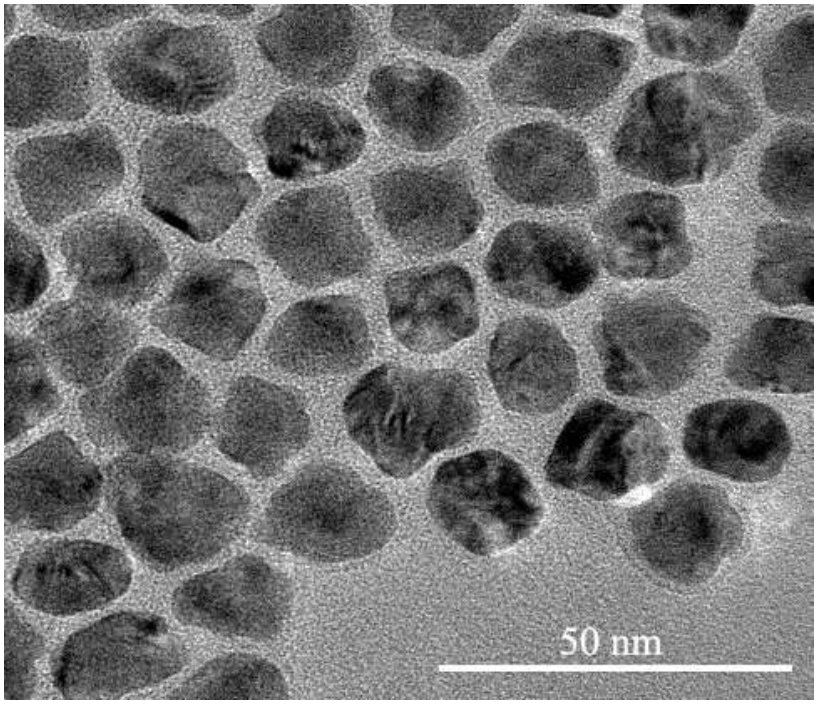

Fig. S1 TEM image of Cu_3PdN.

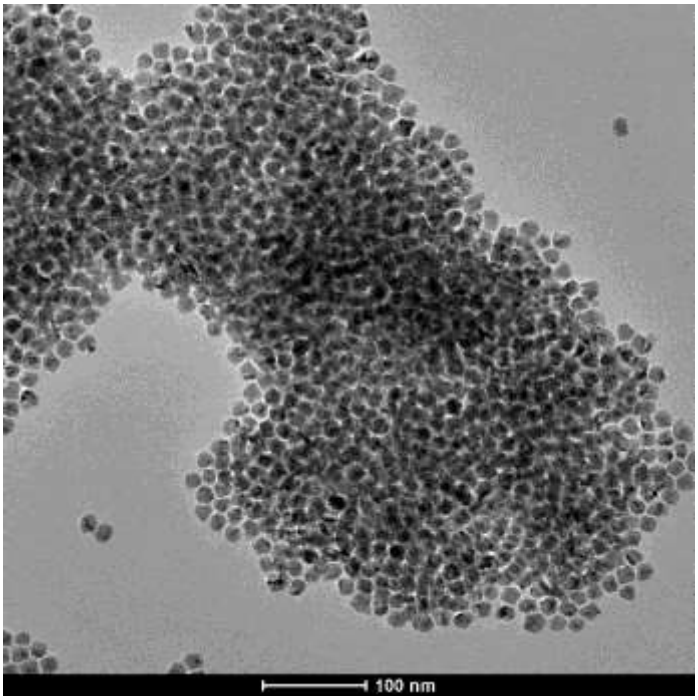

Fig. S2 TEM image of Cu_3N nanoparticles.

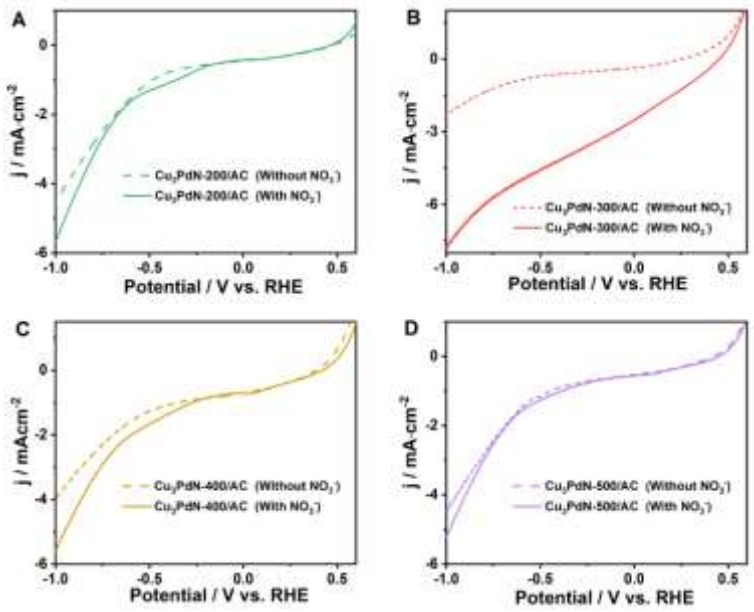

Fig. S3 LSV curves of (**A**) Cu_3PdN-200/AC, (**B**) Cu_3PdN-300/AC, (**C**) Cu_3PdN-400/AC and (**D**) Cu_3PdN-500/AC in Na_2SO_4 with and without 50 ppm $NO3^-$.

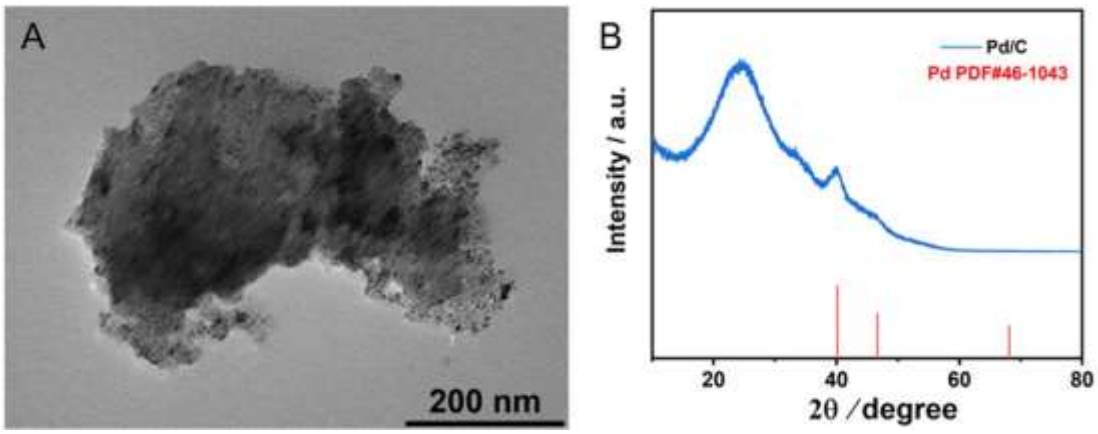

Fig. S4 (**A**) TEM image and (**B**) XRD pattern of commercial Pd/C.

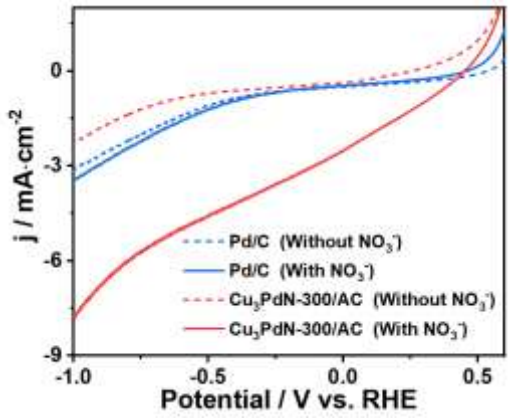

Fig. S5 Comparison of electrocatalytic activities of Cu_3PdN-300/AC and commercial Pd/C in Na_2SO_4 with and without 50 ppm NO_3^-.

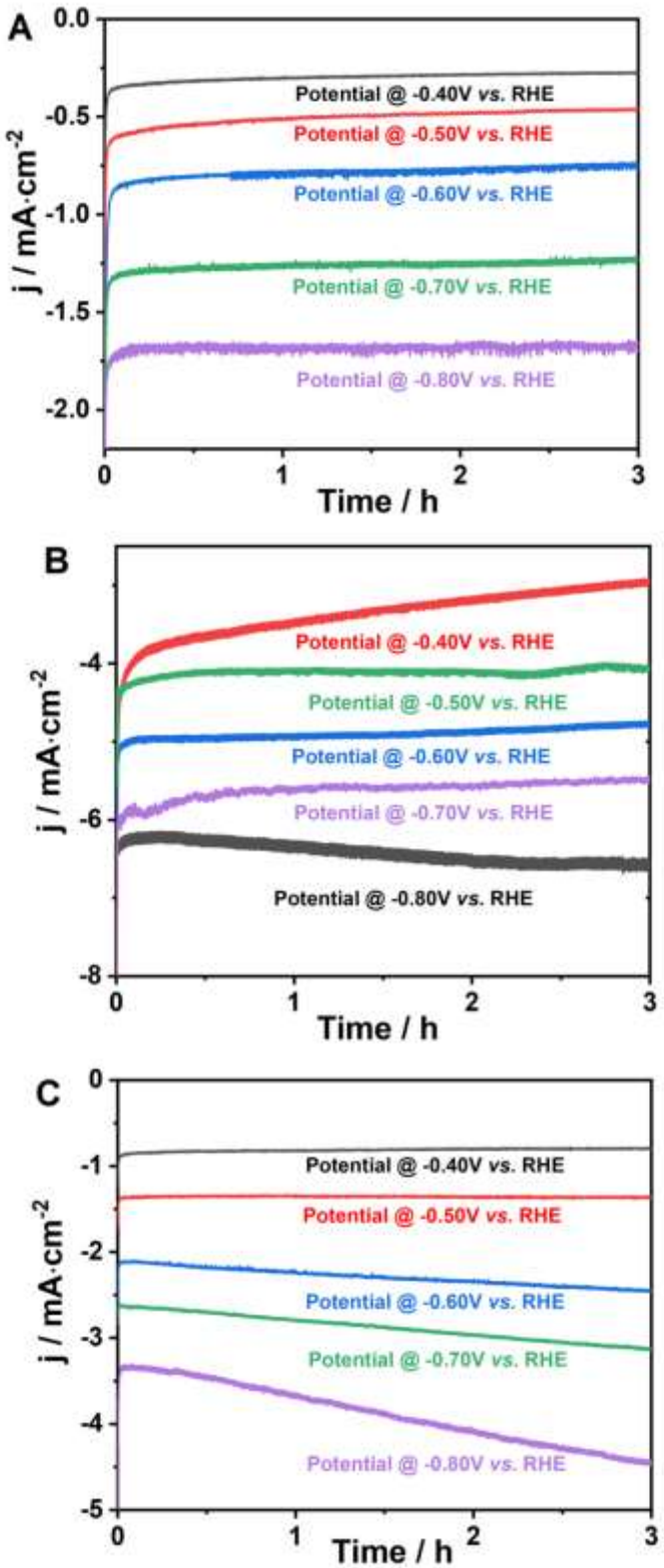

Fig. S6 The *i*-t curves of (**A**) Cu_3N-300/AC, (**B**) Cu_3PdN-300/AC and (**C**) Pd/C at different potential.

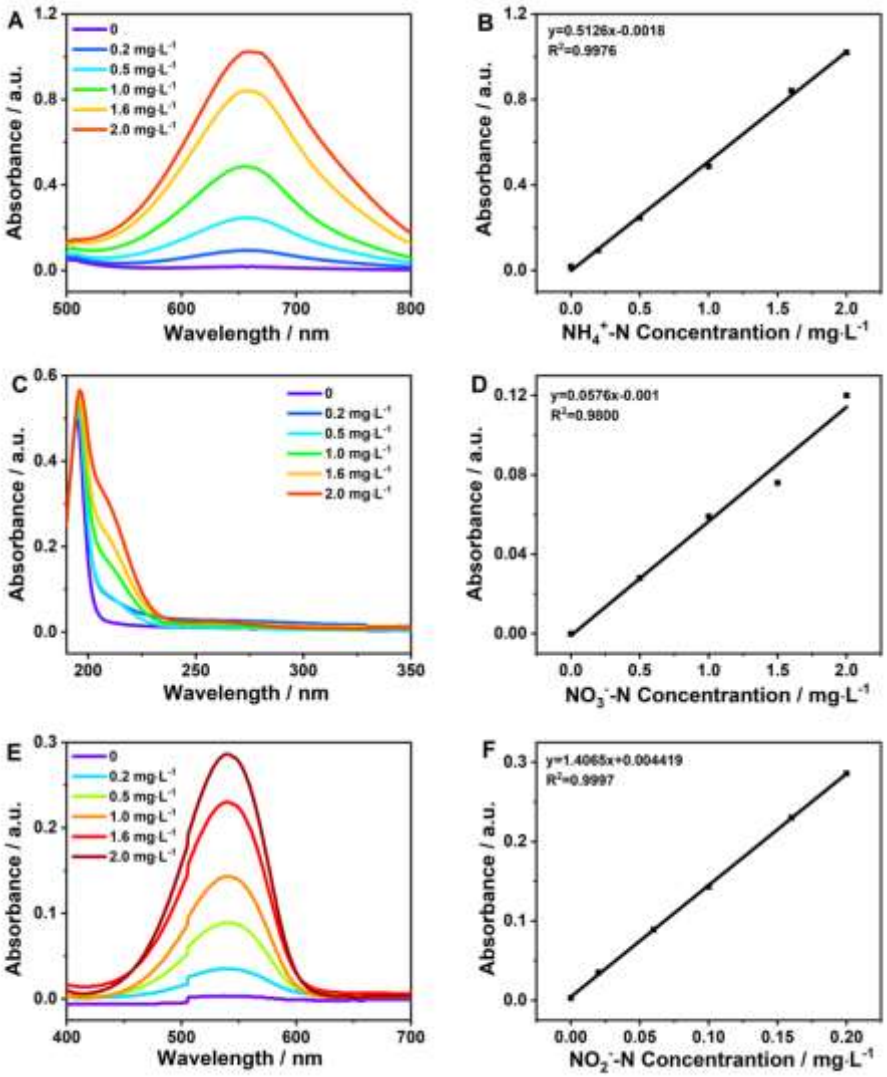

Fig. S7 (**A**) The UV-Vis absorption spectra of NH_4Cl solutions with different concentrations, (**B**) the standard calibration curve for the determination of ammonia; (**C**) The UV-Vis absorption spectra of KNO_3 solutions with different concentrations, (**D**) the standard calibration curve for the determination of NO_3^--N; (**E**) The UV-Vis absorption spectra of KNO_2 solutions with different concentrations, (**F**) the standard calibration curve for the determination of NO_2^--N.

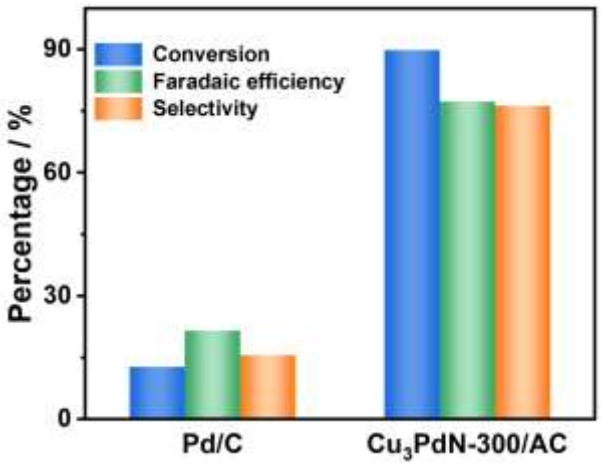

Fig. S8 Faradaic efficiency and selectivity of ammonia and conversion rate of nitrate over Cu_3PdN-300/AC and commercial Pd/C.

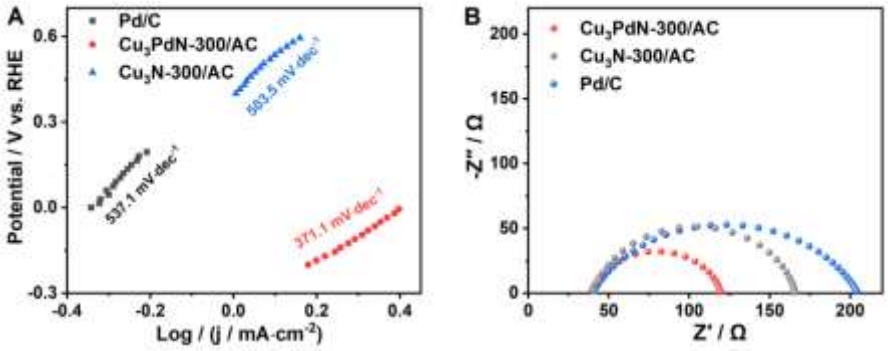

Fig. S9 (**A**) The Tafel slope of Cu_3PdN-300/AC, Cu_3N-300/AC and Pd/C in Na_2SO_4 with $NaNO_3$, (**B**) Nyquist curves for Cu_3PdN-300/AC, Cu_3N-300/AC and Pd/C.

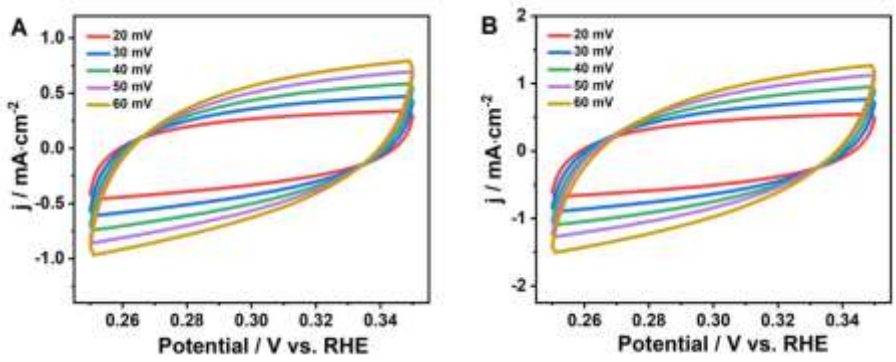

Fig. S10 The CV curves of (A) Cu_3N-300/AC and (B) Cu_3PdN-300/AC at different scan rates.

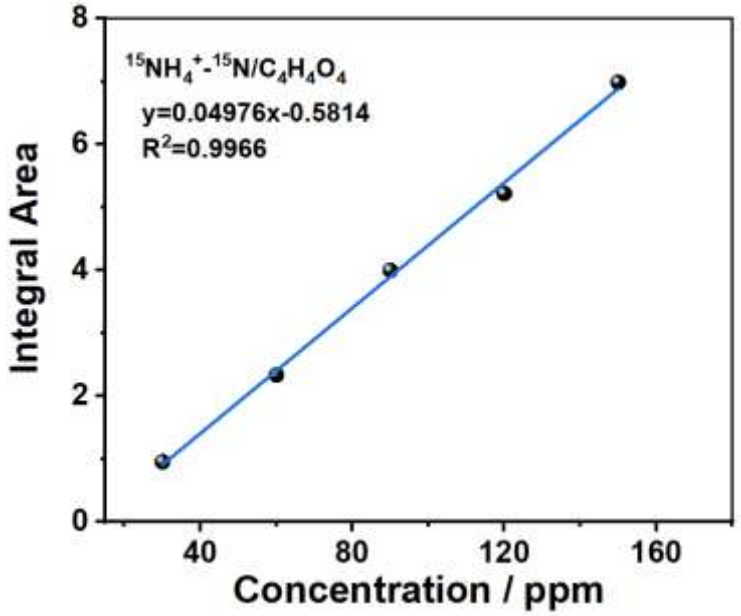

Fig. S11 Standard calibration curve of $^{15}NH_4^+$.

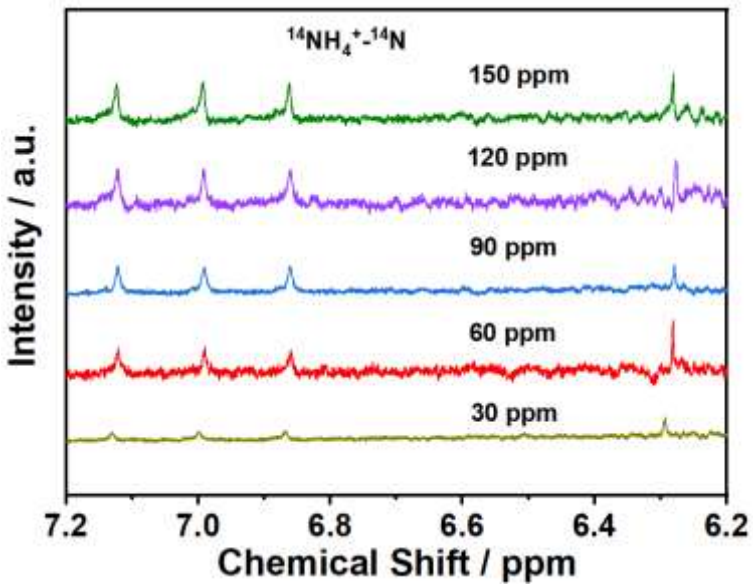

Fig. S12 ^{1}H NMR spectra of the standard $^{14}NH_4^+$ solutions with different concentrations.

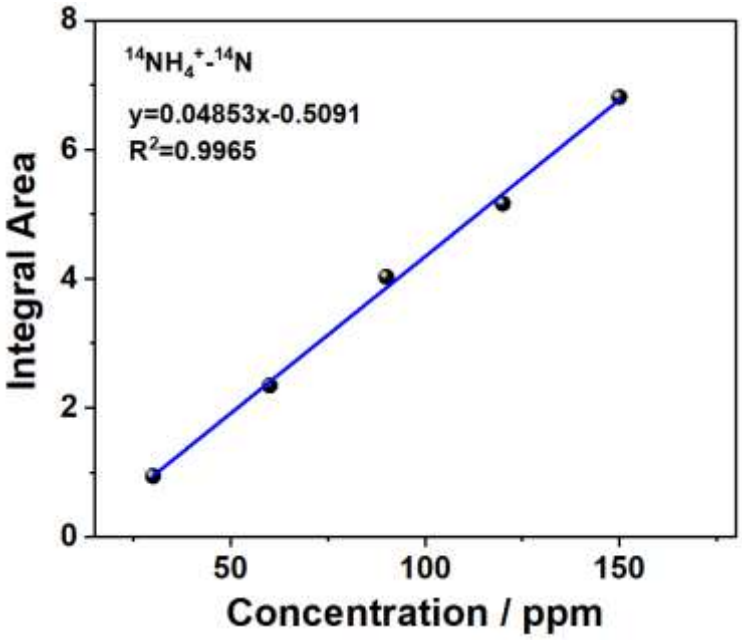

Fig. S13 Standard calibration curve of $^{14}NH_4^+$.

Table S1. Comparison of ammonium synthesis from nitrate electroreduction over Cu_3PdN-300/AC with other reported catalysis.

Catalysis	Electrolyte	Yield rate of NH_3	S_{NH_3}	FE_{NH_3}	Ref.
Cu_3PdN-300/AC	**50 ppm NO_3^- + 1.0 g L^{-1} Na_2SO_4**	**0.10 mmol h^{-1} mg_{cat}^{-1}**	**76.3%**	**77.3%**	**This work**
Co_3O_4/Ti mesh	100 g L^{-1} KNO_3 + 0.1 M K_2SO_4	0.854 mmol h^{-1} mg_{cat}^{-1}	33.6%	1.23%	2
Co_3O_4@NiO	200 ppm NO_3^- + 0.5 M Na_2SO_4	0.00693 mmol h^{-1} mg_{cat}^{-1}	62.29%	54.97%	3
$PdMoCu_{0.5}$	0.1 M KNO_3^- + 1 M KOH	0.254 mmol h^{-1} mg_{cat}^{-1}	-	56.95%	4
$Pd_{0.4}Cu_{0.6}$	0.8 mM NO_3^- + 0.01 M $NaClO_4$	0.0002 mmol h^{-1} mg_{cat}^{-1}	49.0%	-	5
$Pd_{10\%}$-$Cu_{2.5\%}$/CeO_2	0.8 mM NO_3^- + 0.05 M Na_2SO_4	0.0019 mmol h^{-1} mg_{cat}^{-1}	37.0%	-	6
CuPd@DCLMCS/CNTs	100 mg L^{-1} NO_3^- + 0.1 M Na_2SO_4	-	5%	36%	7
PdCu@OMC	8 mM NO_3^- + 0.1 M Na_2SO_4	0.0053 mmol h^{-1} mg_{cat}^{-1}	24.5%	-	8
Pd–Cu/γAl_2O_3	50 ppm NO_3^-	0.0091 mmol h^{-1} mg_{cat}^{-1}	19.6%	-	9
Pd-Cu/SS	0.6 mM NO_3^- + 0.01 M $NaClO_4$	-	6%	-	10
BDD	50 ppm NO_3^- + 0.1 g L^{-1} Na_2SO_4	-	8.9%	42%	11
CuO-Co_3O_4/Ti	100 mg L^{-1} NO_3^- + 0.05 M Na_2SO_4	-	44%	54.5%	12
FeN-NC-140	1.6 mM NO_3^- + 0.1 M Na_2SO_4	0.0001/0.00004 mmol h^{-1} mg_{cat}^{-1}	<10.0%	-	13
Cu/rGO/GP	20 mM NO_3^- + 20 mM NaCl	0.0145 mmol h^{-1} mg_{cat}^{-1}	19.4%	-	14
Fe0@Fe_3O_4	0.8 mM NO_3^- + 0.4 M NaCl	0.0009 mmol h^{-1} mg_{cat}^{-1}	<20%	-	15
CuO_x	50 ppm NO_3^- + 0.1 M KOH	0.024 mmol h^{-1} mg_{cat}^{-1}	-	74.18%	16
Blended $Sn_{0.8}Pd_{0.2}$/SS	0.008 M $NaNO_3$ + 0.1 M $HClO_4$	0.0013 mmol h^{-1} mg_{cat}^{-1}	14%	-	17
Ni-Fe^0@Fe_3O_4	50 ppm NO_3^- + 10 mM NaCl		10.4%	-	18
CL-Fe@C	1.6 mM NO_3^- + 0.1 M Na_2SO_4	0.0007/0.00018 mmol h^{-1} mg_{cat}^{-1}	58%	-	19
Fe SAC	0.5 M KNO_3 + 0.1 M K_2SO_4	0.46 mmol h^{-1} mg_{cat}^{-1}	69%	75%	20

References

1. D. D. Vaughn II, J. Araujo, P. Meduri, J. F. Callejas, M. A. Hickner and R. E. Schaak, *Chem. Mater.*, 2014, **26**, 6226−6232.

2. Y. Wang, Y. Yu, R. Jia, C. Zhang and B. Zhang, *Natl. Sci. Rev.*, 2019, **6**, 730−738.

3. Y. Wang, C. Liu, B. Zhang and Y. Yu, *Sci. China Mater.*, 2020, **63**, 2530−2538.

4. X. J. Tong, Z. W. Zhang, Z. Y. Fang, J. H. Guo, Y. Zheng, X. L. Liang, R. P. Liu, L. T. Zhang and W. Chen, *J. Phys. Chem. C*, 2023, **127**, 5262−5270.

5. J. F. Su, I. Ruzybayev, I. Shah and C. P. Huang, *Appl. Catal. B: Environ.*, 2016, **180**, 199−209.

6. C. Chen, H. Zhang, K. Li, Q. Tang, X. Bian, J. N. Gu, Q. Cao, L. Zhong, C. K. Russell, M. Fan and J. Jia, *J. Catal.*, 2020, **392**, 231−243.

7. H. Xu, J. Wu, W. Luo, Q. Li, W. Zhang and J. Yang, *Small*, 2020, **16**, e2001775.

8. J. Fan, H. Xu, M. Lv, J. Wang, W. Teng, X. Ran, X. Gou, X. Wang, Y. Sun and J. Yang, *New J. Chem.*, 2017, **41**, 2349−2357.

9. Z. Q. Zhang, Y. P. Xu, W. X. Shi, W. Wang, R. J. Zhang, X. Bao, B. Zhang, L. Li and F. Y. Cui. *Chem. Eng. J.*, 2016, **290**, 201−208.

10. H. Ji, P. Du, D. Zhao, S. Li, F. Sun, E. C. Duin and W. Liu, *Appl. Catal. B Environ*, 2020, **263**, 118357.

11. P. Kuang, K. Natsui and Y. Einaga, *Chemosphere*, 2018, **210**, 524−530.

12. M. Yang, J. Wang, C. Shuang and A. Li, *Chemosphere*, 2020, **255**, 126970

13. J. Wang, L. Ling, Z. Deng and W. X. Zhang, *Sci. Bull.*, 2020, **65**, 926−933.

14. D. Yin, Y. Liu, P. Song, P. Chen, X. Liu, L. Cai and L. Zhang, *Electrochim. Acta*, 2019, **324**, 134846.

15. Z. A. Jonoush, A. Rezaee and A. Ghaffarinejad, *J. Clean. Prod.*, 2020, **242**, 118569.

16. J. Geng, S. Ji, H. Xu, C. Zhao, S. Zhang and H. Zhang, *Inorg. Chem. Front*., 2021, **8**, 5209–5213.

17. F. Yao, Q. Yang, Y. Zhong, X. Shu, F. Chen, J. Sun, Y. Ma, Z. Fu, D. Wang and X. Li, *Water Res.*, 2019, **157**, 191−200.

18. Z. A. Jonoush, A. Rezaee and A. Ghaffarinejad, *J. Clean. Prod.*, 2020, **242**, 118569.

19. L. Su, D. Han, G. Zhu, H. Xu, W. Luo, L. Wang, W. Jiang, A. Dong and J. Yang, *Nano Lett.*, 2019, **19**, 5423−5430.

20. Z. Y. Wu, M. Karamad, X. Yong, Q. Huang, D. A. Cullen, P. Zhu, C. Xia, Q. Xiao, M.Shakouri, F. Y. Chen, J. Y. Kim, Y. Xia, K. Heck, Y. Hu, M. S. Wong, Q. Li, I. Gates, S. Siahrostami and H. Wang, *Nat. Commun.*, 2021, **12**, 2870.

Author contributions:

Kai Yao: Investigation, Data curation, Formal analysis, Writing–original draft. **Zhaobin Fang**: Investigation, Data curation. **Jieyue Wang**: Investigation. **Wenhai Wang**: Formal analysis, Revise the draft. **Mingyue Wang**: Formal analysis. **Wenjie Yan**: Investigation. **Mingfu Ye**: Formal analysis. **Binbin Jiang**: Conceptualization, Writing-review & editing. **Konglin Wu**: Conceptualization, Writing–original draft, Supervision. **Xianwen Wei**: Writing–original draft.